Water Desalination Plant Fault Detection using Artificial Neural Network

Maris Murugan T. [1,*] and Kiruba Shankar R. [2]

[1*]Department of Electronics and Instrumentation Engineering, Erode Sengunthar Engineering College, Perundurai, Erode, Tamil Nadu, 638 057, India.

[2]Department of Electronics and Communication Engineering, KPR Institute of Engineering and Technology, Coimbatore, Tamil Nadu, 641 407, India

[*]Corresponding author: T. Maris Murugan

E-mail: marismurugare@gmail.com

GRAPHICAL ABSTRACT

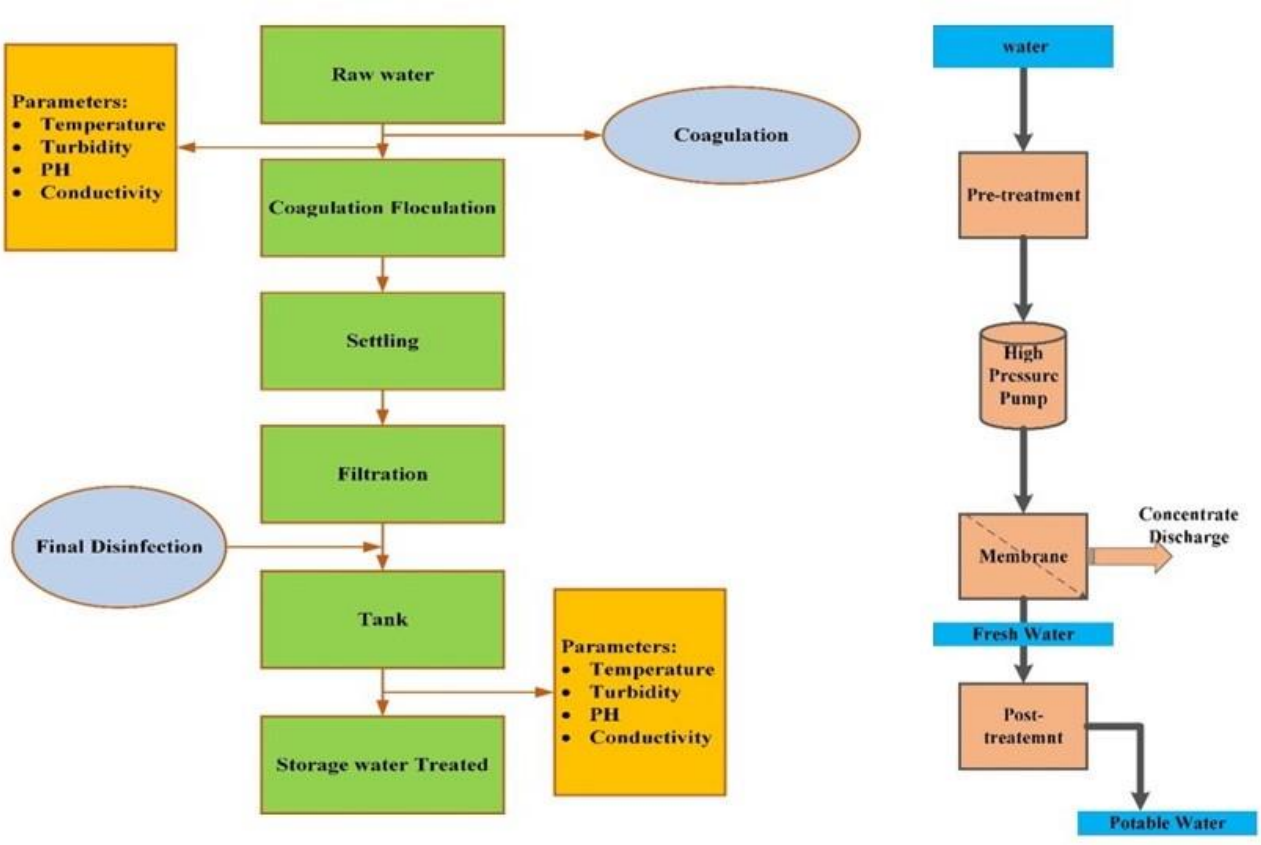

ABSTRACT

Global demand for freshwater has led to increased use of industrial seawater desalination plants. A failure of any component of a desalination plant's control system can result in a malfunction. The fault occurring in the desalination plant slows down the processing speed and reduces the output rate. To overcome these issues, this paper presents an Artificial Neural Network with single and double

component faults (ANN S-DCF) to detect the faults occurring in the desalination plant. The faults are split into two categories and the characteristics of each fault are trained in the ANN. The faults like not under system control, electrical fault, pump fault, control valve fault, inaccurate signal, old data fault, derived fault, and transmitter fault is analyzed here. The result of this work achieves the best accuracy compared to the existing techniques of SVR (Support Vector Regression), PCA (Principal Component Analysis), and DPLS (Dynamic Partial Least Square) method. As a consequence, the proposed ANN technique produces an accuracy rate of 97.04%, a precision rate of 93%, and a sensitivity rate of 95% respectively with low complexity and high operational speed than the existing techniques.

Keywords: Artificial neural network, Desalination plant, Fault, Single and double component fault, Chlorination plant.

1. Introduction

The scarcity of a certain amount of fertile water is increasing, which is essential for life on earth and economic and social development, and environmental sustainability (Gambier, A. et al. 2009). Over the last half-century, enormous advances in saltwater desalination and water treatment technologies have arisen. Even countries that do not have water shortages now may face more water shortages in the future (Ahn, S.J, et al. 2008). The two basic seawater desalination techniques are distillation and membrane separation. To handle the increasing need for freshwater, MSF (Multi-Stage Flash Distillation), MEE (Multi-Effect Evaporation) distillation, VC (Vapour Compression), and RO (Reverse Osmosis) are all the various technologies involved in desalination (Pascual, X, et al. 2014). Figure 1 depicts the basic outlook of the desalination process.

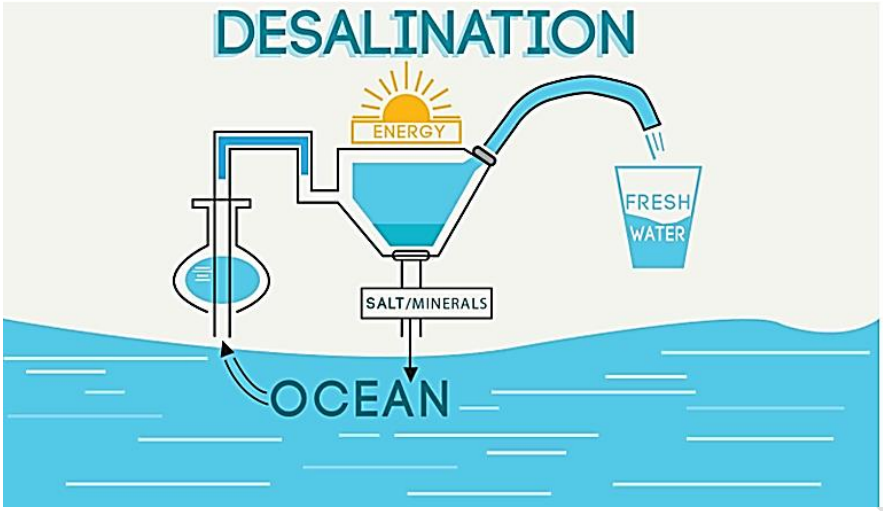

Figure 1. basic outlook of desalination

A desalination plant generally adds chlorine to the intake water to prevent biofouling, which results in the formation of hypochlorite, a toxic gas and mainly hypobromite (Gambier, A, et al. 2010). The most frequently used scrubbing solutions are sodium hydroxide solutions. It is necessary to understand all aspects of chlorine scrubbing applications, including temperature, end products, clearance of the finished products, and the safe handling of all chemicals involved (Sallami, A. et al. 2010; Khawaji, A.D. et al. 2008). It is designed to clean gaseous seepages by scrubbing chlorine from them. The resulting solution must be properly treated and vented to an environmentally responsible place. Many disruptions and defects can be arising during the regular functioning of the desalination system, which is complicated (Achbi, M.S. et al. 2020). The types of faults occurring in the desalination plants such as inaccurate signal, irregular pump working faults, electrical faults, control valve faults, old data faults, and transmitter faults. PCA (principal component analysis) (Garcia-Alvarez, et al. 2011) is applied to observing and identifying malfunctions that occur in the reverse osmosis plant. The monitoring and control of RO plant parameters have been subjected to several efforts, but there have still been challenges, including early fault prediction of different events. As well as early fault detection is among the essential needs for Indian RO plant operators to ensure that the overall plant's life span is extended while maintaining optimal operating conditions as well. Therefore, a proper fault diagnosis technique is needed for a desalination plant.

The paper presents an Artificial Neural Network (ANN) with the single and double component fault (ANN S-DCF) introduced to detect the faults in chlorination plants. First, the faults are categorized into two namely single-component faults and double-component faults. Then, the characteristics or features of each fault are trained in an ANN and this network detects the types of faults.

The remaining content is ordered as the following sections: section 2 establishes the previous techniques of fault detection of the desalination plants; section 3 explains the comprehensive concept of the proposed ANN S-DCF; section 4 described the performance analysis and comparative analysis and section 4 describes the conclusion and the future scope.

2. Related Works

This section provides an overview of various deep learning or machine learning techniques to detect the malfunctions of the seawater desalination system.

Derbali et al., (2017) developed a decision tree algorithm technique to detect the malfunction of a desalination plant. Based on specific measurements, an authentic system was constructed using the membrane distillation system and nanotechnology. The faults that occurred between the model results and system outputs were then categorized to detect system failures.

Abdel Fatah et al., (2018) proposed condition-based maintenance (CBM) method utilized for selecting the appropriate maintenance process in the seawater reverse osmosis desalination system to demonstrate whether digital models may be utilized to provide condition-based monitoring of rising force rising in pumps in a saltwater desalination plant. Because of internal resistance, it might be difficult to execute.

Srivastava, S. et al., (2018) developed a different ANN-based algorithm that can be used with a smartphone-based android app for early fault diagnosis and predictive maintenance and Web-based interfaces for data visualization and analytics. A variety of plant parameters are monitored including

the flow rate, pressure, pH, TDS, and over- and undersupply voltage for the feed and output water tanks.

Wang, B. et al., (2019) proposed a method for detecting Membrane Distillation Systems (MDS) faults using various machine-learning approaches. It was noted that the classification accuracy obtained by using the decision trees was the best as compared to the other learning techniques like K-Nearest Neighbours, Neural Networks, and Support Vector Machines (SVM).

Mehrad, R., and Kargar., (2020) has been introduced a parity space approach for controlling and detecting the faults of the reverse osmosis desalination plant. Here, the parity space approach is utilized to identify the flaws that occur in the actuator. The retreating predictive control-bounded data uncertainties controller is a strong and constant variation of generalized predictive control that is used in the suggested method.

Pérez-Zuñiga et al., (2020) introduced a structural analysis approach in fault detection and isolation (FDI) utilized at any defect in its elements in the control system might cause a system to collapse, posing safety issues, wasting energy, and affecting the quality of freshwater. The analysis of the structural model enables the creation of this system, which may be used to develop diagnostic procedures. But here the sensors are adequately varying depending on the temperature, so a high range of false positive cases will occur.

Mamandipoor, B. et al., (2020) proposed This paper proposes a Deep Neural Networks (LSTM)-based fault model for oxidation and nitrification processes in wastewater treatment plants. A continuous effort is being made to improve the purification performance of WWTPs while at the same time reducing their energy consumption. This has led to an increase in the automation of these plants and, subsequently, an increase in the number of measurement sensors.

Anter, A.M., et al., (2020) proposed a Whale Optimizing Algorithm (WOA), based on chaos theory and fuzzy logic to the identification of faults during wastewater treatment to reduce costs and

validate decision rules, as well as to identify non-well-structured domains in a dataset. The reliability and stability are low by using this method.

This section gives a clear vision of the previous fault detection methods for detecting the malfunctions that occur internally in the desalination system. The major limitations deemed for the previous methods include a low number of faults only detected, taking more time to process, and poor accuracy. To overcome these limitations, the proposed method implements a fault detection technique introduced by a machine learning method including an Artificial neural network (ANN S-DCF) with single and double component faults.

3. Proposed Model:

In this proposed method, the chlorination plant system contains an automatic reader, which automatically takes the readings of the working speed, timing, flow rate, fault rate, and overflow in certain microseconds continuously. It has a lot of working data in a specified time. But, here taking some sets of data with time for processing. The datasets are collected and the features of faults are also trained in an ANN. The combined help of single component faults and double component faults are involved to categorize the features of the faults. The proposed method (ANN S-DCF) is utilized to identify the faults occurring in the chlorination plant shown in Figure 2.

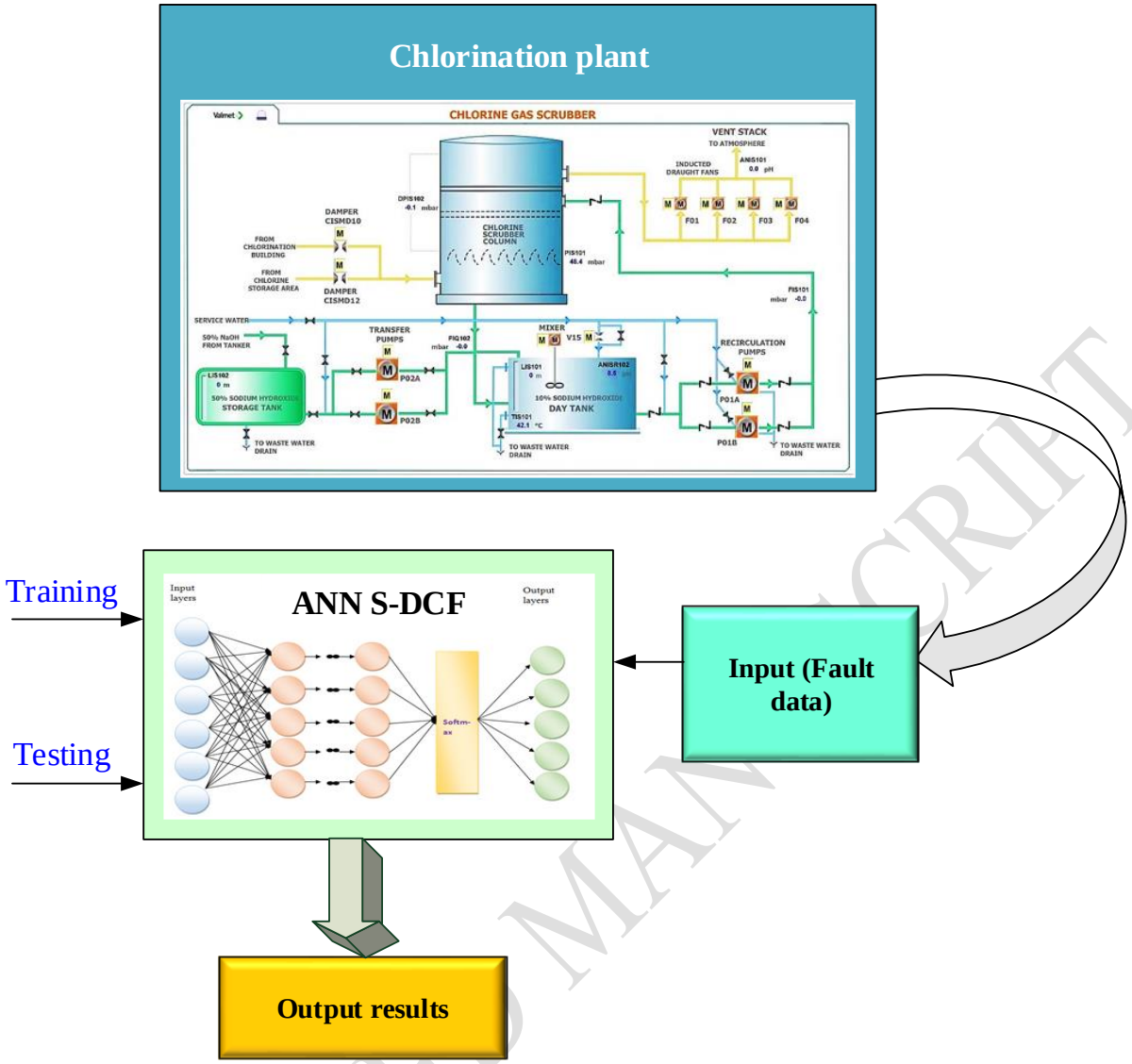

Figure 2. Block diagram of a proposed model

3.1 Chlorination plant:

The emergency chlorine gas scrubber system is intended to safely neutralize unplanned chlorine leaks in the chlorination building and the chlorine storage area (Agus, E. et. Al., 2010). Here, it is considered part of the site's safety equipment and must be maintained and inspected to ensure that it will function properly in an emergency. This chlorine scrubber system is automated, although there is a manual override to start or stop individual pumps, fans, and mixers as needed. While operation, a 10 percent of sodium hydroxide (NaOH) solution is delivered to the top of the scrubber column through an ETA-designed distributor, which ensures equal dispersion of the solution across the packing surface. Once chlorine comes into touch with the caustic solution, it undergoes a quick,

irreversible chemical reaction, removing almost 99.5 percent of the chlorine by the time the gas reaches the top of the column.

From a separate day tank, a 10% of sodium hydroxide (NaOH) solution circulated the column (Verbeke, R. et. Al., 2020). The induced draught (ID) fan is designed to keep the furnace at negative pressure by sucking the combustion products out of it while maintaining a little rising force at the chimney's outflow end. Because of the positive pressure, the exhaust gas leaves the chimney and combines with the surroundings, which is facilitated by the stack effect of the heating chimney at 120°C. The dampers are also a part of this plant, which are automatically regulated and keep within a safe margin of the predicted burner outflow (Farhat, N. et. Al., 2022). The four induced draught (ID) Fans pull chlorine gas through the scrubber column when a chlorine leak is detected in the chlorination facility or the chlorine storage area.

3.1.1 High chlorine detection of chlorine storage area:

When the chlorine storage area sends a high chlorine signal, the scrubber plant's Large Combustion Plants (LCP) activate the specified duty recirculation pump and wait 10 seconds for the lower flow rate switch to activate. If the lower flow rate switch is not activated within that certain interval of time, the duty pump will be turned off and the standby pump will be turned on. Afterward, the HVAC (heating, ventilation, and air supply) control panel will turn on two extracting fans and their corresponding dampers, while the scrubber plant's LCP will turn on two ID (induced draught) fans and wait for twenty seconds for the scrubber column intake pressure to return to normal, if not the system would be shut off. The plant will continue to run till the excessive chlorine alert has been cleared and the fans and pump have been turned off.

3.1.2 High chlorine detection of chlorination building area:

When the chlorine storage area sends a high chlorine signal, the scrubber plant's LCP activates the specified duty recirculation pump and waits for 10 seconds for the lower flow rate switch to activate.

If the lower flow rate switch is not activated within that certain interval of time, the duty pump will be turned off and the stand-by pump will be turned on. Afterward, the HVAC (Heating, Ventilation, And Air Supply) control panel will turn on five extracting fans and their corresponding dampers, while the scrubber plant's LCP will turn on four ID fans and wait for twenty seconds for the scrubber column intake pressure to return to normal, if not the system would be shut off. The plant will continue to run till the excessive chlorine alert has been cleared and the fans and pump have been turned off.

In an auto shut-down sequence, the scrubber system is disabled, and the working pump and fans are halted however when the emergency push button on the local control panel is pressed.

In a caustic fill sequence, the caustic fill process will begin through the chosen duty transferring pump whenever the low level in the storage tank is not enabled. The standby pump will automate to begin the process if the duty pump is disrupted by an electrical problem. When the High level in Day tank or the Low level in the Storage tank is triggered, the caustic filling process is terminated.

3.2 Types of faults occur in the chlorination plant:

The various types of faults occur in the chlorination plant. But here consider the seven types of faults. They are inaccurate fault, external fault, not under system control, Control disabled, old data fault, derived fault, and invalid fault. Fault bits are used to highlight problems in the signal processing chain, starting at the transmitter. They can detect many errors at the same time.

(i) Inaccurate signal fault (f_1):

It can arise based on irregular reading. The signal is reached whenever before or after a certain time, but not transmitted the signal in the corresponding time.

(ii) External fault(f_2):

Fault in the transmitter or signal wire. If more than 420mA means, fault will have occurred. If less than 420 mA means, fault be acquired.

(iii) Not under system control(f_3):

This system will be automatically ON/OFF.

(iv) Control disabled (f_4):

The signal will have come from DCS to the actuators. There is some fault in an actuator. While problems are occurring here.

(v) Old data fault (f_5):

The system will be hanged, the previous value is not valid. The reading is frozen with old values.

(vi) Derived fault (f_6):

One or more of the input signals of a derived signal is faulty

(vii) Invalid fault (f_7):

The signal value is not based on any measurement.

3.3 Single and double component fault (SCF and DCF):

In a single-component fault, the fault should depend on one component, and in a double-component fault in which the fault depends on more than one component. Figure 3 depicts the categorization of faults. The inaccurate signal fault is under the SCF, it depends only on the time. It is represented as f_1.

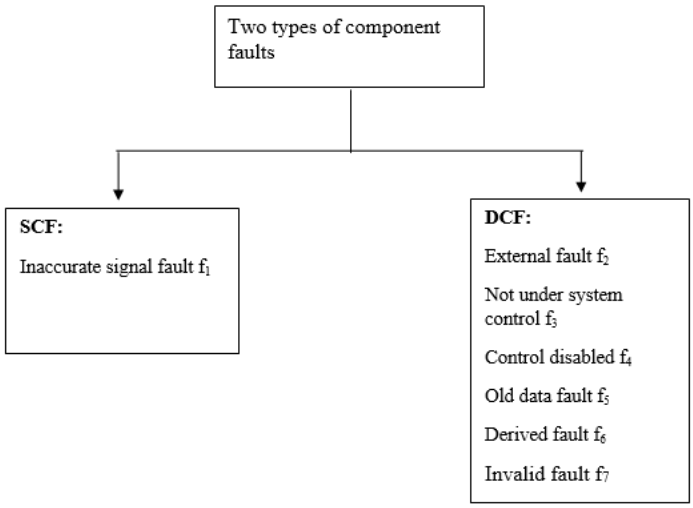

Figure 3. Categorization of faults

The external fault is under DCF, it depends on both less than or greater than 420 mA. It is represented as f_2. The not under-system control fault is under the DCF, it depends on both systems ON/OFF. It is

represented as f_3. The control disabled fault is under the DCF, it depends on DCS and actuators. It is represented as f_4. The old data fault is under the DCF, it depends on the present and past values. It is represented as f_5. The derived fault is under the DCF, it depends on the greater number of faults. It is represented as f_6. The invalid fault is under DCF, it depends on any measurement.

3.4 Working of ANN

An Artificial Neural Network (ANN) is a network of neurons that uses a non-linear transformation to learn highly complicated functions. It has been successfully used for complex categorization tasks like image and signal recognition. Here, ANN is to address fault detection and classification challenges. First, trained the characteristics of the faults such as inaccurate signal fault (f_1), external fault (f_2), not under system control (f_3), control disabled (f_4), old data fault (f_5), derived fault (f_6) and invalid fault (f_7) by using the ANN with various hyperparameter values. Then, look at the impacts of two hyper-parameters on the performance of the ANN including the number of hidden layers and the number of neurons in the last hidden layer. Finally, tested the ability of ANN to classify the faults.

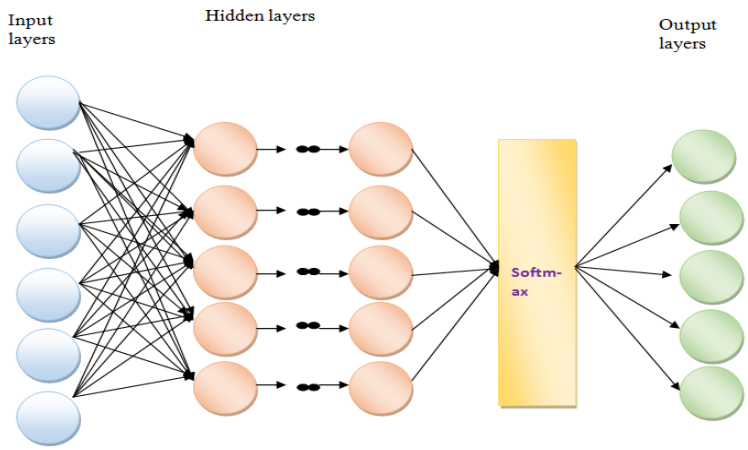

Figure 4. Structure of ANN

Figure 4 demonstrates the four types of layers such as input layer, hidden layer, softmax layer, and output layer (Wu, et. al., 2018). In the fault detection approaches, input data must be normalized before being fed into the input layer and one way to do so is to use the feature scaling of the following

form to ensure that all values are in the range [0, 1]. The representation of scaling is expressed in equation 1.

$$v' = \frac{v - \min imum(v)}{\text{maximum}(v) - \min imum(v)} \quad (1)$$

In the hidden layers, through the following nonlinear transformations, the information provided in the input data is sequentially changed into higher representations like features. The representation of the first and last hidden layer is expressed in equations 2 and 3.

$$H_1 = \sigma(w_1\, u + B_1) \quad (2)$$

$$H_l = \sigma(w_l\, h_{l-1} + B_l),\ l = (2, \ldots\ldots, z) \quad (3)$$

Whereas, u ∈ R^{n_u} , $H_l \in R^{n_{H_l}}$ are the vectors of input and hidden layers representation. Then, $w_l \in R^{n_{H_l} \times n_{H_{l-1}}}$ and $B_l \in R^{n_{H_l}}$ are the weight matrices and bias vectors respectively and z denotes the number of hidden layers. Here, n_{H_l} is represented as the number of neurons present in each hidden layer and σ is a non-linear activation function that makes the above transformation to be non-linear. The rectified linear equation is defined as equation 4.

$$\sigma(u) = \max(0, u) \quad (4)$$

The output of the final hidden layer is subjected to the transformation described in equation (2) without the activation function expressed in equation (5).

$$H_s = w_s\, H_z + B_s \quad (5)$$

In the softmax layer, involves the softmax function of the following equation (6) determines the values of each output neuron.

$$Y_i = \frac{\exp(H_{s,i})}{\sum_{i=1}^{n_{H_S}} \exp(H_{s,i})} \quad (6)$$

The networks next choose the label with the highest output values to apply a predictable label to the input data and to detect the faults as f_1, f_2, f_3, f_4, f_5, f_6, and f_7. The performance analysis and comparative analysis are seen in the result section.

4. Result and Discussion:

This section analyzes the various faults like f_1 (inaccurate signal fault), f_2 (electrical fault), f_3 (pump fault), f_4 (control fault), f_5 (old data fault), f_6 (derived fault), and f_7 (transmitter fault) and trained in ANN S-DCF to detect and classify the faults. For batch training, training datasets are split into twenty-five batches and the networks are trained for two hundred training epochs. The batch size is referred to as the number of training samples utilized in one iteration. The output performance has been estimated, analyzed, and compared to the existing classification approaches. The comparison is made based on the variations in existing and proposed techniques.

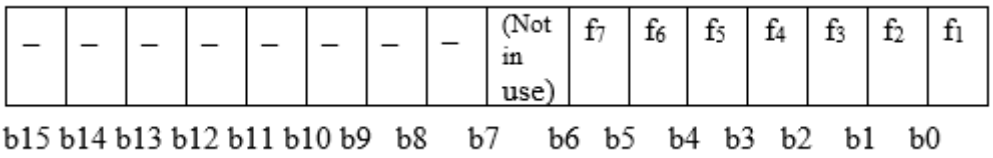

Figure 5: Bit Representation of a fault

4.1 Performance metrics:

The accuracy, precision, sensitivity, and specificity were involved to estimate the outcome of the experiment.

Accuracy:

Accuracy is a parameter shows that the percentage of categorized faults in each class related to the total number of faults in that class. In equation implies the accuracy of the ANN S-DCF.

$$\text{Accuracy} = \frac{number\ of\ samples\ with\ correct\ label}{total\ number\ of\ samples} \tag{7}$$

Precision:

Precision is a parameter that depicts the percentage of detecting the count of positive samples to the total count of positive samples. Equation (8) implies the formula for p_e (precision). Here, p_e (Precision) is calculated by the tp (true positive) outcomes reduced by the total of tp (true positive) and fp (false positive) outcomes.

$$p_e = \frac{tp}{tp+fp} \tag{8}$$

Sensitivity:

It is used to effectively interpret a positive result. It is estimated by analyzing the proportions of the true positives in both fault and functioning cases. The sensitivity is expressed below;

$$\text{Sensitivity} = \frac{tp}{tp+fn} \tag{9}$$

Specificity:

Specificity can detect normal functioning cases. It is used here to identify the negative outcome in the analysis.

$$\text{Specificity} = \frac{tn}{tn+fp} \tag{10}$$

Overall, the proposed model achieves 97.04% accuracy. Figure 6 and Figure 7 show training and testing accuracy and loss curves. The accuracy curve has five to fifty epochs on the x-axis and accuracy on the y-axis as shown in Figure 6. ANN S-DCF's training and testing accuracy curves show a high level of accuracy at 0.9704 based on epochs. On the x-axis of Figure 7 is the loss curve of the ANN S-DCF, whereas the loss on the y-axis is the number of epochs. In both the training and testing phases, its loss is 2.96, which indicates the ANN S-DCF performs well.

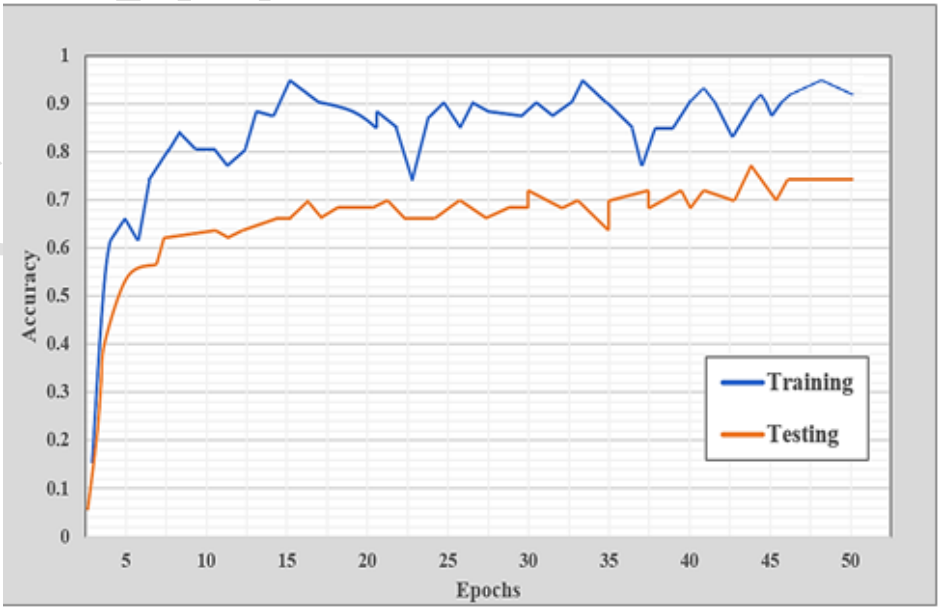

Figure 6: Training and testing accuracy of ANN S-DCF

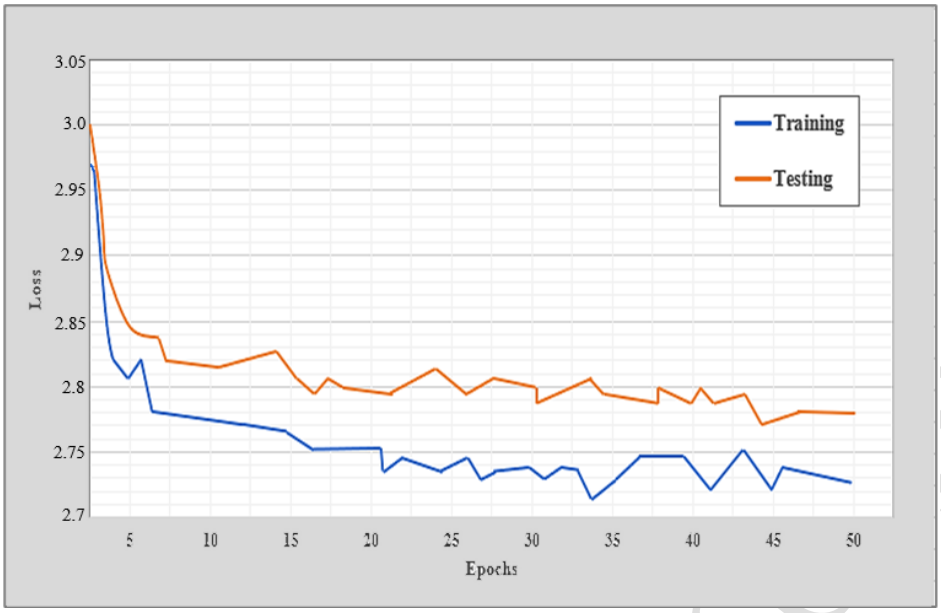

Figure 7: Training and testing loss of ANN S-DCF

Figure 8 depicts the performance of the proposed ANN S-DCF model. The result shows the proposed ANN S-DCF provided an accuracy of 97.05%, precision of 94.32%, specificity of 91.1%, and sensitivity of 92.13%.

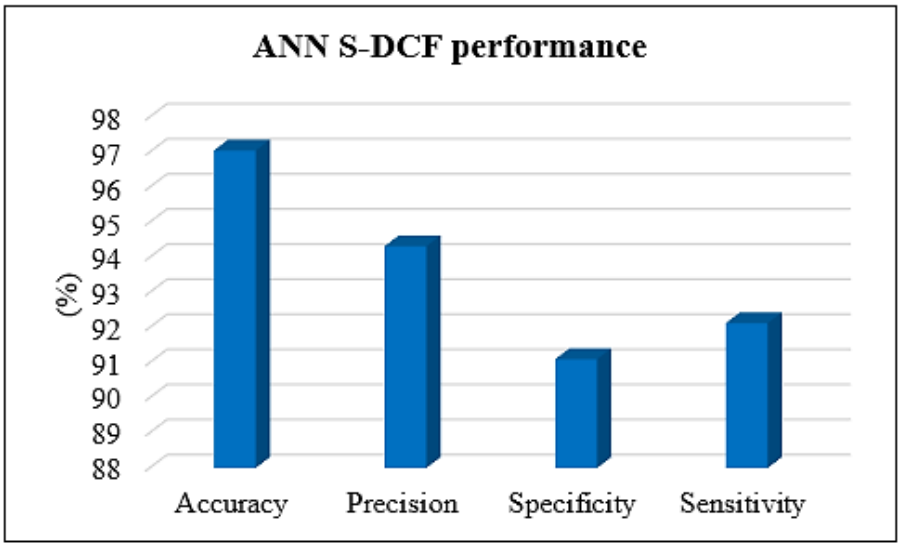

Figure 8: Performance of ANN S-DCF

4.2 Comparative analysis:

The comparison of existing and proposed fault detection methods is replicated in table 1 along with the related graphical representation in figure 9.

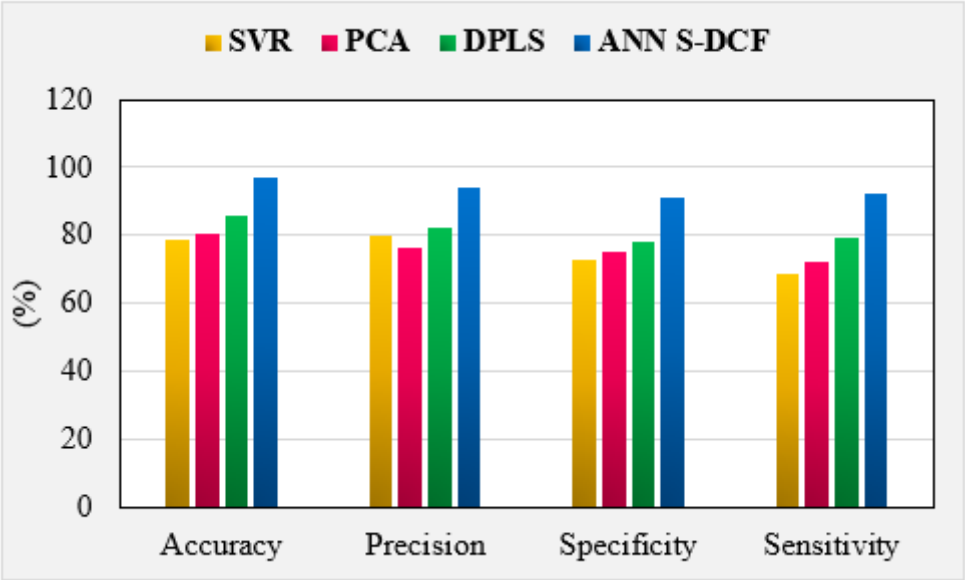

Figure 9: Graphical representation of comparing existing with the ANN S-DCF method

Table 1. Comparison of the ANN S-DCF and existing method

Methods	Accuracy	Precision	Specificity	Sensitivity
SVR	78.5	79.9	72.5	68.83
PCA	80.3	76.3	75.2	72.1
DPLS	85.6	82.13	78.01	79.5
ANN S-DCF	97.05	94.32	91.1	92.13

The performance metrics in percentage are compared to the proposed ANN S-DCF with the existing techniques including (SVR) support vector regression, PCA (principal component analysis), and DPLS (dynamic partial least square). When comparing the accuracy rates of fault detection with existing techniques like (SVR) support vector regression has an accuracy of 78.5 %, principal component analysis (PCA) has an accuracy of 80.3 %, dynamic partial least square (DPLS) has an accuracy of 85.6 %, and the proposed artificial neural network with the single and double component fault (ANN S-DCF) has the maximum accurate of 97.0.5 %. While comparing the precision rate of fault detection with existing techniques like support vector regression (SVR) has a precision rate of

79.9 %, principal component analysis (PCA) has a precision rate of 76.3 %, dynamic partial least square (DPLS) has a precision rate of 82.13 % and the proposed ANN S-DCF reaches the maximum precision rate of 93.32%. Next, comparing the specificity rate in percentage of various fault detection with existing techniques like support vector regression (SVR) has a specificity rate of 72.5 %, principal component analysis (PCA) has a specificity rate of 75.2 %, dynamic partial least square (DPLS) method has a specificity rate of 78.01 % and the proposed ANN S-DCF reaches the specificity rate of 92.1%. Then, comparing the sensitivity rate in percentage of various fault detection with existing techniques like support vector regression (SVR) has a sensitivity rate of 68.83 %, principal component analysis has a sensitivity rate of 72.1 %, dynamic partial least square (DPLS) method has the sensitivity rate of 79.5 % and the proposed ANN S-DCF reaches the sensitivity rate of 95.13 %. The proposed ANN S-DCF reaches the maximum accuracy and highly reliable than the other existing systems.

5. Conclusion:

The primary intent of this study is to split the various types of faults according to the depending component with single-component faults and double-component faults. After, that the features are trained to the artificial neural network (ANN). The proposed ANN S-DCF can be trained in all possible ways to detect and classify the faults like inaccurate signal fault (f_1), external fault (f_2), not under system control (f_3), control disabled (f_4), old data fault (f_5), derived fault (f_6) and invalid fault (f_7) with low error rate. It deeply learned the features of each fault and reaches the maximum accuracy of training and testing data. This system quickly detects the faults and diagnose them with a minimum number of misclassification rate. The output values of the proposed ANN S-DCF fault detection are compared with the different fault detection techniques, to check the advancement of the proposed method. Within the instance of identifying the malfunctioning, researchers looked at the impact of two factors (number of hidden layers, number of neurons in the last hidden layer) on system performance and discovered that, beyond a definite point, increasing network size does not improve fault identification accuracy rate. The proposed system has the benefit of being simple and efficient

for industrial sectors. This proposed framework achieves an accuracy of 97.05%, a precision rate of 94% and specificity rate of 92.13 %, and a high computational speed. This work will encourage the use of Deep Neural Networks both in chlorination plants and in IoT-based Distributed Control Systems (DCS).

References

Gambier, A., Blumlein, N. and Badreddin, E., June (2009), Real-time fault tolerant control of a reverse osmosis desalination plant based on a hybrid system approach, *In 2009 American Control Conference IEEE*, St. Louis, MO, USA, 1598-1603.

Ahn, S.J., Lee, C.J., Jung, Y., Han, C., Yoon, E.S. and Lee, G., (2008), Fault diagnosis of the multi-stage flash desalination process based on signed digraph and dynamic partial least square, *Desalination*, **228**, 68-83.

Pascual, X., Gu, H., Bartman, A., Zhu, A., Rahardianto, A., Giralt, J., Rallo, R., Christofides, P.D. and Cohen, Y., (2014), Fault detection and isolation in a spiral-wound reverse osmosis (RO) desalination plant, *Industrial & Engineering Chemistry Research*, **53**, 3257-3271.

Gambier, A., Miksch, T. and Badreddin, E., (2010), June. Fault-tolerant control of a small reverse osmosis desalination plant with feed water bypass, *In Proceedings of the 2010 American Control Conference* IEEE, Baltimore, MD, USA, 3611-3616.

Sallami, A., Mzoughi, D. and Mami, A., (2018), Diagnosis of reverse osmosis desalination water system using bond graph approach, *Turkish Journal of Electrical Engineering & Computer Sciences*, **26**, 1638-1650.

Khawaji, A.D., Kutubkhanah, I.K. and Wie, J.M., (2008), Advances in seawater desalination technologies, *Desalination*, **221,** 47-69.

Achbi, M.S. and Kechida, S., (2020), Methodology for monitoring and diagnosing faults of hybrid dynamic systems: a case study on a desalination plant, *Diagnostyka*, **21**, 27-33.

Garcia-Alvarez, D., Fuente, M.J. and Palacin, L.G., December (2011), Monitoring and fault detection in a reverse osmosis plant using principal component analysis, *In 2011 50th IEEE Conference on Decision and Control and European Control Conference IEEE*, Orlando, FL, USA, 3044-3049.

Derbali, M., Fattouh, A., Jerbi, H. and Abdelkrim, M.N., (2016), Improved fault detection in water desalination systems using machine learning techniques, *Journal of Theoretical & Applied Information Technology*, **92,** 380

Abdel Fatah, A., Lofty, M., Hassan, M. and Dimitri, A., (2018), Using Digital Models for Condition Based Maintenance of High-Pressure Pumps in SWRO Desalination Plants, In Asia Turbomachinery & Pump Symposium, 2018 Proceedings. *Turbomachinery Laboratory, Texas A&M Engineering Experiment Station.*

Srivastava, S., Vaddadi, S., Kumar, P. and Sadistap, S., 2018. Design and development of reverse osmosis (RO) plant status monitoring system for early fault prediction and predictive maintenance. *Applied Water Science*, *8*(6), pp.1-10.

Wang, B., Li, Z., Dai, Z., Lawrence, N. and Yan, X., 2019. A probabilistic principal component analysis-based approach in process monitoring and fault diagnosis with application in wastewater treatment plant. *Applied Soft Computing*, *82*, p.105527.

Mehrad, R. and Kargar, S.M., 2020. Integrated model predictive fault-tolerant control, and fault detection based on the parity space approach for a reverse osmosis desalination unit. *Transactions of the Institute of Measurement and Control*, *42*(10), pp.1882-1894.

Pérez-Zuñiga, G., Rivas-Perez, R., Sotomayor-Moriano, J. and Sánchez-Zurita, V., (2020), Fault Detection and Isolation System Based on Structural Analysis of an Industrial Seawater Reverse Osmosis Desalination Plant, Processes, **8**, 1100.

Mamandipoor, B., Majd, M., Sheikhalishahi, S., Modena, C. and Osmani, V., (2020), Monitoring and detecting faults in wastewater treatment plants using deep learning, *Environmental monitoring and assessment*, **192,** 1-12.

Anter, A.M., Gupta, D. and Castillo, O., 2020. A novel parameter estimation in dynamic model via fuzzy swarm intelligence and chaos theory for faults in wastewater treatment plant. *Soft Computing*, *24*(1), pp.111-129.

Agus, E. and Sedlak, D.L., 2010. Formation and fate of chlorination by-products in reverse osmosis desalination systems. *Water research*, *44*(5), pp.1616-1626.

Verbeke, R., Eyley, S., Szymczyk, A., Thielemans, W. and Vankelecom, I.F., 2020. Controlled chlorination of polyamide reverse osmosis membranes at real scale for enhanced desalination performance. *Journal of Membrane Science*, *611*, p.118400.

Farhat, N., Kim, L., Mineta, K., Alarawi, M., Gojobori, T., Saikaly, P. and Vrouwenvelder, J., 2022. Seawater desalination-based drinking water: Microbial characterization during distribution with and without residual chlorine. *Water Research*, *210*, p.117975.

Wu, Y.C. and Feng, J.W., 2018. Development and application of artificial neural network. *Wireless Personal Communications*, *102*(2), pp.1645-1656.

Figures

Figure 9: Graphical representation of comparing existing with the ANN S-DCF method

Tables

Table 1. Comparison of the ANN S-DCF and existing method